Condensed Matter Physics, 2002, Vol. 5, No. 2(30), pp. 227–247

CONDENSED MATTER PHYSICS

Towards a simplified approach to the modelling of the star-like molecule fluids

Yu.Duda [1,2] , A.Trokhymchuk [2,3]

[1] Programa de Ingenieria Molecular, Instituto Mexicano del Petróleo, Eje Central L.Cardenas 152, 07730, México D.F.

[2] Institute for Condensed Matter Physics of the National Academy of Sciences of Ukraine, 1 Svientsitskii Str., 79011 Lviv, Ukraine

[3] Department of Chemistry and Biochemistry, Brigham Young University, Provo, UT 84602, USA

Received March 29, 2002

A theoretical approach to considering a wide spectrum of equilibrium properties of fluids formed from the four-branched molecules (e.g. four-arm star polysterene samples, four-arm block copolymers, etc.) is presented and discussed. The proposed approach is within the framework of an associative version of integral equation theory and is based on an analytical solution of the four-site associative hard-sphere model. Results and discussion are explained by the comparison against Monte Carlo computer simulation data generated for a freely-joined tangent hard-sphere model of a star-like molecule fluid. It is shown that the proposed theory works well for the star-like molecule fluids in homogeneous phase where it predicts the structure for molecules with relatively long arms and at high densities. The obtained results qualitatively reproduce the most important experimental features of the solvation force induced between two macrosurfaces due to the presence of star-like aggregates.

Key words: *star-like molecules, associative integral equation theory, computer simulation*

PACS: *05.20.Jj, 61.25.Em*

1. Introduction

In recent years much attention has been paid to the modeling and studying various properties of branched polymers. One special class of branched polymers that has recently received considerable attention from both theoretical scientists and engineers is the star-like molecule (SLM) fluid or star polymers [1–19]. The

SLM fluid[1] serves as a prototype example for tethered chains, polymer brushes, and multibranched systems. Depending on the extension, the SLM aggregates can be viewed as molecules or macromolecules, where more than two linear homopolymers, which are called arms, are all chemically attached to a common microscopic seed. The size of the seed is typically of the order of a bond length, i.e. significantly smaller compared to the extension of the chain. The existence of the seed seems to be the most important factor for the special identity of SLM fluids within the entire family of polymers. The star molecules are also related to other objects such as colloidal particles (in the limit of infinitely large number of arms) or linear polymer chains (in the case when the number of arms is equal to one or two).

Besides experimental investigations of the branched polymers [1–7], computer modeling, analytical and semi-analytical statistical-mechanics treatments provide a valuable way of understanding these systems at a fundamental level [8–19]. However, an exact statistical-mechanics treatment of branched molecules, in general, is complicated because of the large number of internal degrees of freedom, the coupled intra- and intermolecular interactions between beads, etc. Thus, it is important to introduce the simplified approaches to such complicated objects and to see if the phenomena observed in the experiments can be reproduced and explained by relatively simple models. Different models of SLM fluid have been developed and various statistical-mechanics techniques have been adopted to study them. Basically, these are very sophisticated approaches such as molecular dynamics (MD) and Monte Carlo (MC) computer simulations [8–12] as well as the mean-field theory methods [13,14], renormalization group analysis [15–17], thermodynamic perturbation theory [18], and scaling theory [19]. Most of these approaches have been devoted to the structure and conformational properties of a single star molecule or to the thermodynamics of the SLM fluid.

The methods of integral equation theory [20–28] in conjunction with computer simulation methods [8–11] seem to be one of the most suitable tools of investigating the dense SLM systems. The information about interstar correlations provided by these techniques may lead to a deeper insight and understanding of the diffraction experimental data on dense star polymer solutions. Computer simulations are the best possibility since the generated data may be considered exact for a given model. Particularly, when the modeling opportunities are practically unlimited. With the development of new generations of computers, inaccuracies introduced by the system size could be overcome though some methodological problems, like space sampling, still exist. The main problem faced by the integral equation theory concerns the appropriate modeling: the model must be reasonably adequate but still has to permit an analytical or at least a numerical (semi-analytical) treatment under certain approximations. An advantage of the integral equation theory is that this approach is significantly less time consuming. Therefore, a promising strategy is to test the theoretical predictions versus computer experiment for some chosen

[1]For an approach outlined in this study as well as for the results and discussions presented, the term "star-like molecule fluids" is more appropriated than "star polymers" and abbreviation "SLM" will be used throughout

conditions and properties and then try to exploit this model under the conditions and for the properties that are difficult to reach by computer modeling.

The main goal of the present contribution is to share with readers a simplified approach to the fluid systems composed of star aggregates. Our consideration includes both the modelling and semi-analytical treatment aspects. The model considered here belongs to the class of the so-called associative hard-sphere models. The theoretical tool for treating such models is a multi-density formalism realized through the associative version of the integral equation theory [22,23]. We will apply this approach to a wide spectrum of properties of the SLM fluids in an homogeneous and inhomogeneous phase and will try to find out how the theoretical predictions are related to both the computer simulations and to the observation. To further proceed with the results and discussion, in the following section we briefly introduce the fundamentals of the theoretical scheme and outline the details of computer simulation procedure.

2. Fundamentals of theoretical approach

2.1. Associative integral equation theory

The theoretical approach employed to study the properties of the SLM fluid is based on the associative version of integral equation theory combined with the four-site associative (FSA) model.

Four-site associative model of the SLM fluid. This model consists of N hard-sphere particles, which we will call beads, in a volume V and of diameter d (without any loss of generality in some parts of our presentation we assume $d = 1$). The particle total number density is defined as $\rho = N/V$. Each of the beads has four interaction spots (or sites) placed on their surface. The sites are of two types, denoted as a and b. Two neighboring beads can form an associative complex (aggregate) due to the site-site ($a-b$) interaction only. Bonding between the same type of sites is not allowed. The mutual location of the sites determines the aggregate conformation, while the strength of the site-site attraction together with the number (density) of beads are responsible for the aggregate space extension. In the present study, we restrict ourselves to the freely-joined formations: attraction sites are randomly located on the bead surface and they are independent of each other, i.e. bonded state of a given site on the bead does not affect a bonding ability of any other site on the same bead.

The pairwise interaction, $U(\mathbf{1},\mathbf{2})$, between two beads, 1 and 2, consists of the centre-centre hard-sphere repulsion plus the site-site attraction and can be written in a form:

$$U(\mathbf{1},\mathbf{2}) = U_{\mathrm{HS}}(r) + \left(\sum_{a,b} U_b^a(\mathbf{1},\mathbf{2}) + \sum_{a,b} U_b^a(\mathbf{2},\mathbf{1}) \right), \tag{2.1}$$

where $\mathbf{1}$ and $\mathbf{2}$ denote the position and orientations of two particles; $U_{\mathrm{HS}}(r)$ is the hard-core interaction between any two particles with r being their centre-to-centre separation; $U_b^a(\mathbf{1},\mathbf{2})$ denotes the potential for a short-range and highly directional

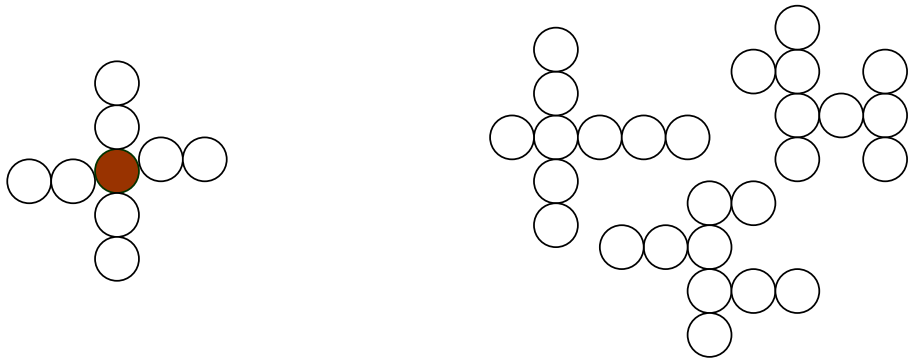

Figure 1. Two-dimensional sketch of the different star-like aggregates that could be formed within the four-site associative (FSA/SLM) model used in WOZ/APY theory (right panel) and the star-like molecule within the tangent hard-sphere (THS/SLM) model employed in MC simulations (left panel).

attraction between site a on particle 1 and site b on particle 2. For the sake of convenience, in what follows we use the superscripts for sites a and the subscripts for sites b.

To provide an analytical treatment of the FSA model, the site-site attraction, $U_b^a(\mathbf{1},\mathbf{2})$, is chosen to be infinitesimally short-ranged so that the corresponding orientation-averaged f-function [26,29] (an associative analog of the classical Mayer function) is proportional to the Dirac δ-function [30]:

$$f_b^a(r) = K_b^a \delta(r-1), \tag{2.2}$$

where K_b^a is the stickiness parameter of the site-site $(a{-}b)$ attraction. At a fixed bead number density, ρ, by an appropriate choice of the stickiness parameter K_b^a, the FSA model could reproduce various types of aggregates, i.e. linear polymers, symmetrical and nonsymmetrical networks *etc.* Recently, some of these possibilities have been studied and analyzed [29,31]. In the present study, we restrict our attention to the case when all site-site interactions are the same, i.e., $K_b^a \equiv K$, that topologically corresponds to a star-like formations. In what follows, we will refer to this model as the FSA/SLM model. The schematic two-dimensional presentation of the FSA/SLM model is shown in figure 1.

Multi-density formalism. FSA/SLM model introduced above belongs to the class of the so-called associative hard-sphere models. The theoretical approach to treat such models is a multi-density formalism realized through the associative version of integral equation theory pioneered by Wertheim [22,23]. According to Wertheim, the division of the potential of interaction (2.1) into an associative and non-associative parts allows one to classify the diagrammatic representation of the grand partition function in terms of the cluster diagrams which account for the formation of the aggregates of various size and conformation. Therefore, the graphs defining the total number density are classified according to the bonded state of the labeled point **1**. Then, the total local number density can be presented as follows:

$$\varrho(\mathbf{1}) = \hat{\varrho}_0(\mathbf{1}) + \hat{\varrho}_G(\mathbf{1}) + \hat{\varrho}_{G'}(\mathbf{1}) + \hat{\varrho}_\Gamma(\mathbf{1}), \tag{2.3}$$

where the captured densities are defined as follows:

$$\hat{\varrho}_0(\mathbf{1}) = \varrho_0^0(\mathbf{1}) + \varrho_0^F(\mathbf{1}) + \varrho_0^{F'}(\mathbf{1}) + \varrho_0^\Gamma(\mathbf{1}), \tag{2.4}$$
$$\hat{\varrho}_G(\mathbf{1}) = \varrho_G^0(\mathbf{1}) + \varrho_G^F(\mathbf{1}) + \varrho_G^{F'}(\mathbf{1}) + \varrho_G^\Gamma(\mathbf{1}), \tag{2.5}$$
$$\hat{\varrho}_{G'}(\mathbf{1}) = \varrho_{G'}^0(\mathbf{1}) + \varrho_{G'}^F(\mathbf{1}) + \varrho_{G'}^{F'}(\mathbf{1}) + \varrho_{G'}^\Gamma(\mathbf{1}), \tag{2.6}$$
$$\hat{\varrho}_\Gamma(\mathbf{1}) = \varrho_\Gamma^0(\mathbf{1}) + \varrho_\Gamma^F(\mathbf{1}) + \varrho_\Gamma^{F'}(\mathbf{1}) + \varrho_\Gamma^\Gamma(\mathbf{1}). \tag{2.7}$$

The function, $\varrho_i^\alpha(\mathbf{1})$, represents the partial densities of the individual bead **1** with a given bonded state of its sites. The diagrammatic analysis similar to that developed in [22–25] leads to the relation of the partial densities, $\varrho_i^\alpha(\mathbf{1})$, with the partial one-particle direct correlation functions, $c_i^\alpha(\mathbf{1})$, which in turn define the corresponding two-particle direct correlation functions:

$$c_{ij}^{\alpha\beta}(\mathbf{1},\mathbf{2}) = \frac{\delta c_i^\alpha(\mathbf{1})}{\delta\sigma_{\Gamma-j}^{\Gamma-\beta}(\mathbf{2})}, \tag{2.8}$$

where $\sigma_{\Gamma-j}^{\Gamma-\beta}(\mathbf{2})$ are the density parameters of labeled point **2**. Two-particle direct correlation functions, $c_{ij}^{\alpha\beta}(\mathbf{1},\mathbf{2})$, are related to the partial pair correlation functions, $h_{ij}^{\alpha\beta}(\mathbf{1},\mathbf{2})$, through an associative version of the Ornstein-Zernike (OZ) equation formulated by Wertheim [22,23] and due to this is abbreviated in present study as WOZ equation:

$$h_{ij}^{\alpha\beta}(\mathbf{1},\mathbf{2}) = c_{ij}^{\alpha\beta}(\mathbf{1},\mathbf{2}) + \sum_{l,m}\sum_{\gamma\varepsilon}\int \mathrm{d}\mathbf{3}\, c_{il}^{\alpha\gamma}(\mathbf{1},\mathbf{3})\sigma_{\Gamma-l-m}^{\Gamma-\gamma-\varepsilon}(\mathbf{3})h_{mj}^{\varepsilon\beta}(\mathbf{3},\mathbf{2}). \tag{2.9}$$

Here and everywhere below, the indices $\{\alpha,\beta,\gamma,\varepsilon\}$ are used to denote the sites of type a while $\{i,j,l,m\}$ are reserved for the sites of type b and are assigned the values 0, F, Γ and 0, G, Γ, respectively.

Density parameters and self-consistency relations. The density parameters, $\sigma_i^\alpha(\mathbf{1})$, are defined as the linear combinations of the partial densities:

$$\sigma_i^\alpha(\mathbf{1}) = \sum_{j=0}^{i}\sum_{\beta=0}^{\alpha}\varrho_j^\beta(\mathbf{1}). \tag{2.10}$$

These parameters have to be evaluated from the self-consistency relations. As a part, these relations include

$$\sigma_{\Gamma-G}^\Gamma(\mathbf{1}) = \varrho(\mathbf{1})X_G(\mathbf{1}); \qquad \sigma_\Gamma^{\Gamma-F}(\mathbf{1}) = \varrho(\mathbf{1})X^F(\mathbf{1}), \tag{2.11}$$

where quantities, $X_G(\mathbf{1})$ and $X^F(\mathbf{1})$, are the fractions of the particles not bonded at sites G and F, respectively. In the case of a star-like topology there is relation: $X_G(\mathbf{1}) = X^F(\mathbf{1})$, and each of the fraction can be calculated as follows:

$$X^a = X_b = 2 \Big/ \left[1 + \sqrt{1 + 32\pi\rho K y_{00}^{00}(r=d)}\right]. \tag{2.12}$$

In this equation, $y_{00}^{00}(r = d)$ is a contact value of the partial cavity correlation function. The partial cavity correlation functions, $y_{ij}^{\alpha\beta}(r)$, are related to the partial radial distribution functions, $g_{ij}^{\alpha\beta}(r)$, by:

$$\begin{aligned} g_{ij}^{\alpha\beta}(r) &= h_{ij}^{\alpha\beta}(r) + \delta_{i,0}\delta_{j,0}\delta^{\alpha,0}\delta^{\beta,0} \\ &= e(r)y_{ij}^{\alpha\beta}(r) + e(r)\sum_{a,b} y_{i,j-b}^{\alpha-a,\beta}(r)f_b^a(r)[1-\delta^{\alpha,0}][1-\delta_{j,0}] \\ &\quad + e(r)\sum_{a,b} y_{i-b,j}^{\alpha,\beta-a}(r)f_b^a(r)[1-\delta_{i,0}][1-\delta^{\beta,0}], \end{aligned} \tag{2.13}$$

where $e(r) = \exp[-U_{\rm HS}(r)/kT]$, while δ_{ij} and $\delta^{\alpha\beta}$ stand for the Kronecker symbol. Solving the set of self-consistency relations given through equations (2.9)–(2.13), one will reproduce all the density parameters required for the solution of equation (2.9).

Approximations applied to solve the WOZ equation. Equation (2.9) is solvable analytically subject to a set of approximations. First of all, an associative analog of the Percus-Yevick (APY) closure is formulated in a form [26]:

$$\begin{aligned} c_{ij}^{\alpha\beta}(r) &= y_{ij}^{\alpha\beta}(r)[e(r)-1] + e(r)\sum_{a,b} y_{i,j-b}^{\alpha-a,\beta}(r)f_b^a(r)[1-\delta^{\alpha,0}][1-\delta_{j,0}] \\ &\quad + e(r)\sum_{a,b} y_{i-b,j}^{\alpha,\beta-a}(r)f_b^a(r)[1-\delta_{i,0}][1-\delta^{\beta,0}]. \end{aligned} \tag{2.14}$$

To proceed further, the ideal network approximation [26,29] is applied. In accordance with this approximation, we neglect the part of the intramolecular correlations responsible for the formation of the ring-like complexes with respect to all $(a-b)$ pairs of the sites. The most developed conformation in such a case is the network consisting of crossing polymer chains built along each of the $(a-b)$ directions and with each polymer branch being described within the ideal chain approximation [24]. Therefore, any pair of atoms in such a network is assumed to remain singly connected with changing particle density or strength of the associative interaction.

The WOZ equation (2.9) together with the APY closure conditions (2.14) and with the density relations (2.10)–(2.12) form a closed set of equations to be solved. We refer to this as the WOZ/APY theory. The method used for the solution is based upon Wertheim-Baxter factorization technique [30,32]. The general scheme of the analytical solution is similar to that presented in [24].

Identification of the star-like aggregates. The size (total number of beads) of the complexes formed in the FSA/SLM fluid is characterized by the mean cluster size:

$$M = \frac{4(4 + X_b - 2X_b^2)}{3(1 - 6X_b + 9X_b^2)}, \tag{2.15}$$

where X_b is the fraction of the beads not bonded at site b and is defined according to equation (2.12). The above expression (2.15) was derived within the percolation theory in [27]. In the present study, we identify M as the number of beads per star-like molecule or as the size of a star-like aggregate. Thus, we assume that $M = \xi m+1$ with ξ being the functionality or number of arms. For the FSA/SLM model ξ is equal to 4. Parameter m is the length of each arm.

2.2. Monte Carlo simulations

Tangent hard-sphere model. The star-like aggregates in computer simulations are modeled as a collection of freely-joined tangent hard spheres (THS) and below we will refer to this model as the THS/SLM fluid (see figure 1). The THS/SLM model of a functionality $\xi = 4$ arms and with $m = 2$, 4 6 and 8 beads per each arm have been simulated at different volume fraction, $\eta = \pi\rho/6$, occupied by star-like aggregates. Number density, ρ, has the same meaning as for the FSA/SLM model and corresponds to the total (arm beads+central beads) number density of beads. The central and arm beads are of the same size. We used no less than 160 star-like molecules that is equivalent to the total number of hard-sphere monomers in the box, $N = (\xi m+1)\times 160$. Some test runs with a larger number of star-like aggregates have been performed but no finite-size effect was observed.

Canonical ensemble simulations. Bulk Monte Carlo (MC) simulations were performed in the canonical ensemble with a cubic simulation cell supplemented by a standard periodic boundary conditions applied in all three directions. In most cases, the initial configurations were generated through the random insertion of a central bead followed by the growth of the rest of a molecule. At high densities the growth cycles have been combined with an attempt to move a randomly chosen molecule and to add one bead to a randomly chosen molecule. Trials have been continued until all star molecules are completely grown to the desired size (desired number of participating beads) [33]. After an initial configuration has been generated, the system is allowed to evolve by moving a randomly chosen single molecule. The scheme is adjusted so that about 30–35% of the attempted moves are accepted. This simulation algorithm corresponds to a slightly modified version of the Dickman-Hall algorithm [34], appropriately adapted to the star molecules. At this stage, a random number of beads, m_x ($m_x \leqslant m$), of each of the arms of a randomly chosen star-like molecule is deleted. Following this, a chain is regrown by adding beads sequentially. In a straightforward application of the Metropolis algorithm [35], trial configurations are accepted if they are free of overlap.

To obtain a fairly smooth radial distribution function, runs of approximately $5 \cdot 10^4$ simulation cycles are required. Additionally, an initial one quarter of this number of cycles is necessary to equilibrate the system. To simulate the non-uniform (near a single wall) SLM fluid, we used the same algorithm but applied to computational cell which is elongated in Z direction, i.e. parallelepipedic in a shape. In this case, the periodic boundary conditions are applied in X and Y directions only. The length of computational cell along Z direction, L_z, was chosen large enough to have the homogeneous (bulk) region in the center of the cell. For the slit-like (between two walls) confinement, the length of computational cell, L_z, was equal to the gap width, H. The density profiles, $\rho(z)$, are calculated in MC runs by counting the number of beads, N_z, in the slabs of thickness, $\Delta z = 0.05$, parallel to the XY plane using $\rho(z) = \langle N_z\rangle/v_0$, where v_0 is the slab volume, $v_0 = L_x L_y \Delta z$, and z is the coordinate of the center of the slab.

3. Results and discussion

The results and discussion presented bellow consist of two main parts. First one is aimed at making comparison between the FSA/SLM model used in theoretical treatment and the THS/SLM model simulated in a computer experiment. The second part concerns the physics beyond the theoretical model of the SLM fluid. To compare the theoretical predictions for the FSA/SLM model with computer simulation data for the THS/SLM model, the attraction parameter, K, that serves as an input in the WOZ/APY theory, was adjusted to make the mean cluster size, M, of the FSA/SLM model equal to the number of beads per star-like molecule employed in MC simulations of the THS/SLM fluid.

3.1. Star-like molecule fluid in a bulk

The bulk properties and an information regarding correlations in the SLM fluid can be analyzed by means of the total radial distribution function and the total structure factor.

Total radial distribution function. One of the most important results provided by the WOZ/APY theory is the total radial distribution function (RDF) of the FSA/SLM model. In particular, by factorizing equation (2.9) and using an iteration method due to Perram [36], the partial radial distribution function, $g_{ij}^{\alpha\beta}(r)$, can be obtained [29]. These partial RDFs are similar to those in Wertheim theory of chemical association [22,23]; they do not have a physical meaning that might follow from the indices (0 – unbonded, F or G – partially bonded and Γ – completely bonded) [20]. However, they are used to calculate the total radial distribution function, $g(r)$, which for the FSA/SLM fluid is the following superposition of the partial functions [26]:

$$g(r) = \frac{1}{\rho^2} \sum_{i,j} \sum_{\alpha,\beta} \sigma_i^{\alpha} g_{\Gamma-i,\Gamma-j}^{\Gamma-\alpha,\Gamma-\beta}(r) \sigma_j^{\beta}. \tag{3.1}$$

Figure 2, as an example, shows the total RDFs resulting from the WOZ/APY theory for the FSA/SLM fluid and from the MC simulations for the THS/SLM fluid. We can see a remarkable qualitative and quantitative agreement between the theoretical results and simulation data between both sets of RDFs for almost all parameters considered. The WOZ/APY theory for the FSA/SLM model agrees better with simulation data for the THS/SLM model at higher densities. Some quantitative disagreement was observed [40] at low densities, ρ, especially for the smaller star entities. Since the ideal network approximation [26,29] employed for the FSA/SLM fluid has the same physical origin as the ideal chain approximation in the case of linear chains [24], the prediction of the WOZ/APY theory is more satisfactory for the stars with longer arms ($m = 6$ in the case of figure 2) similar to its greater success for the longer linear chains [24]. Fortunately, the case of longer arms is of utmost interest with a view to future applications of the WOZ/APY theory to inhomogeneous problems.

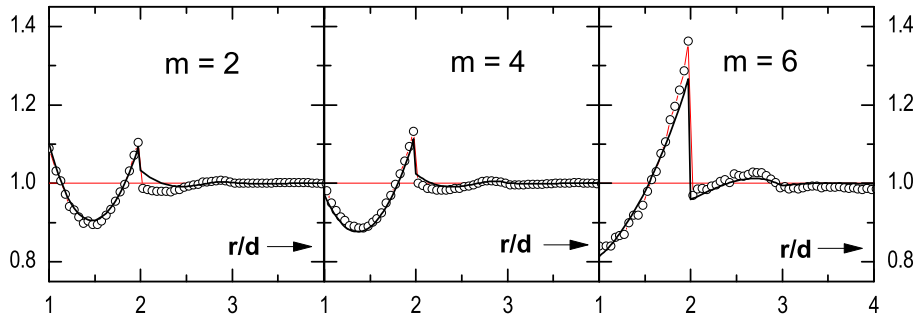

Figure 2. Total radial distribution function, $g(r)$, of a four-armed star-like molecule fluid with various arm length, m, indicated in the figure. Number density of fluid beads is fixed at $\rho = 0.5$. The solid lines and symbols correspond to WOZ/APY theory results for the FSA/SLM model and MC data for the THS/SLM model, respectively.

Structure factor. A knowledge of the total RDF enables us to calculate the total structure factor, $S(k)$, which is related to the Fourier transform of $g(r)$ as follows:

$$S(k) = 4\pi\rho \int [g(r) - 1] \frac{\sin kr}{kr} r^2 \mathrm{d}r. \tag{3.2}$$

However, evaluation of $S(k)$ for the SLM fluid from the definition (3.2) by numerical integration is not the most productive way. Due to the long-range nature of the density fluctuations in the SLM fluid and due to the discontinuity-like behavior of $g(r)$ at $r \approx 2d$ (depicted by both FSA/SLM and THS/SLM model fluids) the accuracy of numerical procedure is questionable. In such a case, an advantage of analytical solution of the FSA/SLM model is evident. Particularly, in present case the structure factor can be calculated implicitly from the knowledge of Wertheim-Baxter factor q-functions as it was discussed in [26].

The resulting structure factor for the total number density of beads fixed at $\rho = 0.5$ is plotted in figure 3. We intend to show the changes in $S(k)$ caused by an increasing of the arm length. It is seen that the curves for arm length, $m = 2, 4$ and 8, differ mainly in the magnitudes of the maxima and minima of $S(k)$. Particularly, the magnitude of oscillations versus wavelength number increases when arms become longer. Another interesting aspect of the results presented in figure 3 is the difference between SLM fluid structure factor and that for the spherical monomer fluid, i.e. for hard-sphere (HS) fluid of the same number density. Besides the shift towards larger k-values in the position of the main peak of $S(k)$ for SLM fluid, the appearance of a new peak (pre-peak) at $1 < kd < 3$ is observed. The genesis of this pre-peak with an increasing arm length reveals its relation to the size of SLM aggregates. More generally, we can conclude that pre-peak is an indication of the density fluctuations due to the formation of the stable structure units with the size larger than the size of basic units, i.e. beads in the case of the SLM fluids.

From the full expression for $S(k)$, its low-k limit can be expressed. The value of $S(k = 0)$ is an important quantity because it is connected with the isothermal

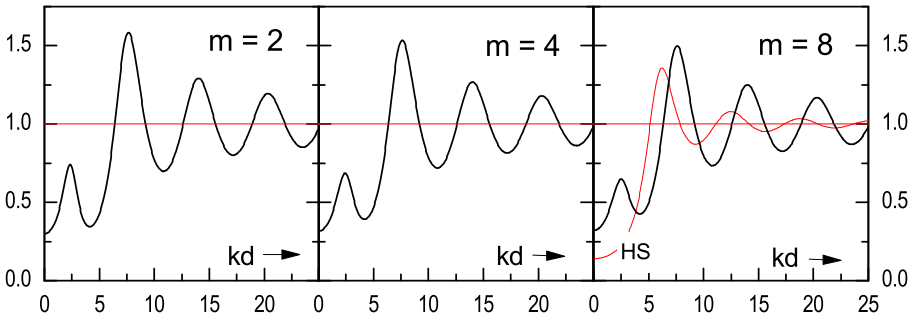

Figure 3. Total structure factor, $S(k)$, of a four armed star-like molecule fluid with different arm length, m, indicated in the figure. Number density of fluid particles (beads) is fixed at $\rho = 0.5$. The solid lines show the results for the FSA/SLM fluid while the thin solid line corresponds to HS fluid.

compressibility by $S(k=0) = \rho kT\chi_T$. Therefore, the behavior of $S(k=0)$ is closely related to the compressibility pressure equation [26].

3.2. Star-like molecule fluid under confinement

The structure of molecular fluids next to the substrate is a subject of great fundamental and technological interest. This topic is connected with many important processes including adsorption, adhesion, manufacturing of thin films, membrane separation, and others. Very little theoretical work has been reported for inhomogeneous properties of SLM fluids. The aim of this section is to get insight both into the ordering of the SLM fluid next to a single wall and into local density of the SLM fluid confined into a space between two rigid surfaces.

HAB approach to modelling a single-wall confinement. Recently, the set of papers was published [28,37] where the classical method developed by Henderson, Abraham and Barker [38] for inhomogeneous hard-sphere fluid had been extended to the inhomogeneous polymerizing fluids. The attractive feature of this approach, which we will abbreviate as the HAB, is a possibility to preserve an analytical treatment without the notable loss of accuracy even for more sophisticated models of adsorbed fluids. A necessary requirement is to know the correlation functions of the same model fluid in the bulk phase.

The planar wall (W) confinement is formed in the HAB approach as a result of a limiting procedure applied to the (SLM fluid plus HS fluid) mixture in which the concentration of hard-sphere particles is taken to tend to zero whereas their diameter tends to infinity. Then, the fluid-wall correlations are described by the associative version of the HAB integral equation [28,39]:

$$h_{j0}^{\alpha \mathrm{W}}(z) = c_{j0}^{\alpha \mathrm{W}}(z) + \sum_{lm} \sum_{\beta,\gamma} \int \mathrm{d}\mathbf{r}' c_{jl}^{\alpha\gamma}(r') \sigma_{lm}^{\gamma\beta} h_{m0}^{\beta \mathrm{W}}(|\mathbf{r} - \mathbf{r}'|), \tag{3.3}$$

where $h_{j0}^{\alpha \mathrm{W}}(z)$ and $c_{j0}^{\alpha \mathrm{W}}(z)$ are the fluid-wall partial pair and direct correlation functions, respectively. Both the density parameters, $\sigma_{lm}^{\gamma\beta}$, and the partial direct corre-

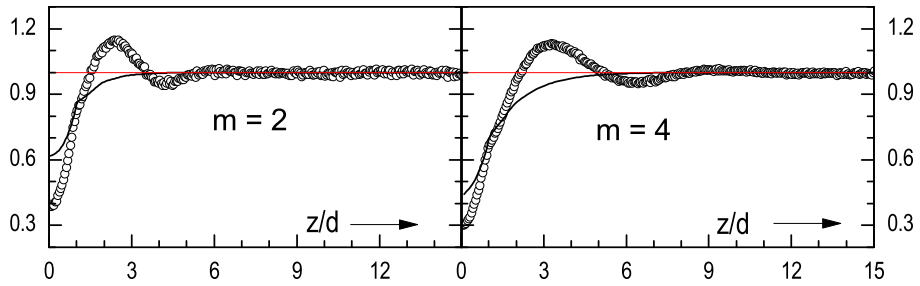

Figure 4. Total normalized density profile, $g_{\rm W}(z)$, of a four-armed star-like molecule fluid next to a hard wall. The arm length, m, is variable as it is indicated in the figure. Bulk number density of fluid particles (beads) is fixed at $\rho = 0.42$. The solid lines and symbols correspond to the WOZ/APY theory results for the FSA/SLM model and MC data for the THS/SLM model, respectively.

lation functions of the bulk fluid, $c_{ij}^{\alpha\beta}(r)$, are the same as those already defined in a previous section.

Similarly to the bulk case, the APY closure is the most popular approximation to solve associative HAB equation (3.3). It reads:

$$g_{j0}^{\alpha{\rm W}}(z) = y_{j0}^{\alpha{\rm W}}(z) + f_{\rm W}(z) y_{j0}^{\alpha{\rm W}}(z); \qquad c_{j0}^{\alpha{\rm W}}(z) = f_{\rm W}(z) y_{j0}^{\alpha{\rm W}}(z), \tag{3.4}$$

where $y_{j0}^{\alpha{\rm W}}(z)$ are the partial cavity-wall correlation functions, $g_{j0}^{\alpha{\rm W}}(z)$ are the normalized partial local densities that are defined through the partial pair correlation functions as follows: $g_{j0}^{\alpha{\rm W}}(z) = h_{j0}^{\alpha{\rm W}}(z) + \delta_{j0}\delta^{\alpha 0}$. Function, $f_{\rm W}(z)$=$\exp[-\beta U_{\rm W}(z)]-1$, is the Mayer function for the bead-wall interaction:

$$U_{\rm W}(z) = \begin{cases} \infty, & \text{if} \quad z < 0 \\ 0, & \text{if} \quad z \geqslant 0, \end{cases} \tag{3.5}$$

where z is the distance between the center of any bead and the wall.

The set of equations (3.3)–(3.4) can be solved analytically in Laplace space by a standard factorization method of reduction to the Baxter q-functions [30,32]. By combining Baxter method with an iteration procedure suggested by Perram [36], the solution for local density distribution could be easy inverted into a real space.

Local density near a single wall. The total normalized local density distribution that incorporates the density of all (arm + central) beads of the star-like aggregates, $g_{\rm W}(z) \equiv \rho_{\rm W}(z)/\rho$, is the following combination of the partial particle densities:

$$g_{\rm W}(z) = g_{00}^{0{\rm W}}(z) + \frac{1}{\sigma_\Gamma^\Gamma} \sum_{i,\alpha} \sigma_i^\alpha g_{\Gamma-i,0}^{\Gamma-\alpha,{\rm W}}(z). \tag{3.6}$$

In order to estimate the relevance of theoretical prediction, in figure 4 we show both the results of equations (3.3)–(3.6) for the FSA/SLM model and MC simulation data for the THS/SLM model. Two models being treated by different theoretical tools result in a quite similar local density behavior. An exception has to be made for the close vicinity of the wall. It is worth noting that we have an interplay of two

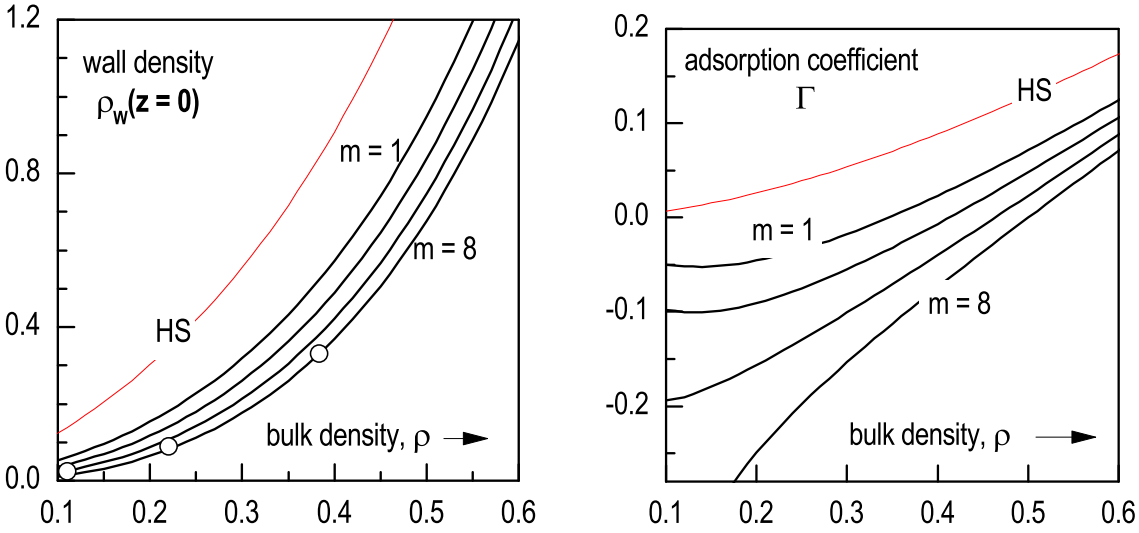

Figure 5. Wall density (left side) and excess surface coverage (right side) of a four-armed SLM fluid next to a hard wall vs. bulk density, ρ. The curves from top to bottom on each part of the figure are the WOZ/APY theory results for the FSA/SLM model of arm length, $m = 1$, 2, 4 and 8. Symbols on the left part are MC simulation data for for THS/SLM model with $m = 2$.

factors which compensate one another: (i) the approximations involved in theoretical treatment (PY approximation and the ideal network approximation) and (ii) the differences in the modelling. Similarly to the homogeneous case, there is a tendency to improve the agreement with an increase of the arm length.

The wall or contact density, $\rho_{\mathrm{W}}(z = 0)$, of the SLM fluid as a function of the bulk number density, ρ, and at various arm lengths is plotted in figure 5. We can see that for the same bulk density, the wall density decreases with the increase of the arm length. In the case of the fluid of spherical molecules, the wall density is always higher than the bulk density. In contrast, for the SLM fluid this is true starting from some certain value of ρ. For example, it corresponds to $\rho = 0.3$ for $m = 1$. However, this density increases with an increase of the arm length, e.g. $\rho = 0.5$ when $m = 8$.

Another property closely related to the wall density is the excess surface coverage defined as follows:

$$\Gamma = \rho \int_0^\infty \mathrm{d}z[g_{\mathrm{W}}(z) - 1] = \rho \lim_{s\to 0} \left[\tilde{g}_{\mathrm{W}}(s) - \frac{1}{s}\right]. \tag{3.7}$$

Very often Γ is called as the adsorption isotherm, adsorption coefficient or excess surface coverage and provides an important overall surface-coveraging characterization of the adsorption. Baxter solution for the Laplace transform, $\tilde{g}_{\mathrm{W}}(s)$, allows to take the limit in equation (3.7) and an analytical expression for Γ is available [28]. The results for Γ in the case of the FSA/SLM fluid vs the bulk density and at different arm length are shown in figure 5 as well. One can see that an excess surface coverage of the SLM fluid is always lower than for HS fluid of the same bulk number density and decreases as the arms become longer. Moreover, the excess

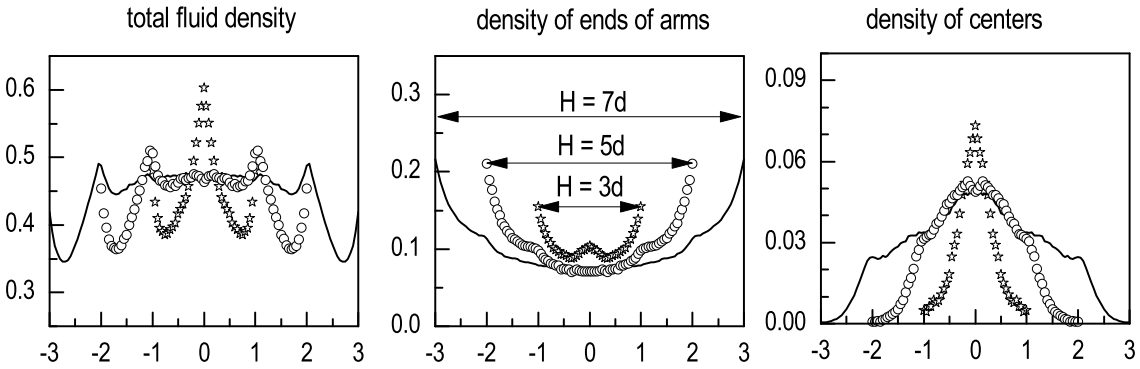

Figure 6. Total fluid local density, local density of the ends of arms and local density of the central beads of the THS/SLM fluid in a slit formed by two hard walls fixed at three different separations: $H = 3d$ (stars); $H = 5d$ (circles) and $H = 7d$ (solid line). Particle number density in the slit defined as the number of all beads devided by the slit volume is fixed at 0.44 in all cases.

surface coverage provided by the fluid of spherical molecules is positive at all bulk conditions, while in the case of the SLM fluid Γ could be negative, especially, at low bulk densities, i.e., low bulk pressures. However, in all cases Γ grows if the bulk fluid becomes denser. This is consistent with the density distributions, particularly, with the depletion effect observed in the behavior of local density in figure 4. We expect that Γ calculated within the WOZ/APY theory works better at low densities. At higher densities the deviations are quite possible. It follows from the fact that the hard-sphere/hard-wall system behaves in that manner.

Local density in a slit formed by two walls. Similarly to the single-wall case, the computer simulation offers a valuable insight into the local ordering of the star-like molecules adsorbed into a space confined by two unmovable surfaces. For simplicity the surfaces are modeled as the hard walls impenetrable to the centers of both the central and the arm beads and only entropic effect of the confinement is considered. Canonical MC simulations for the slit geometry were performed at conditions when the total number density of beads in each pore is maintained the same. Since simulation cell is not connected with the reservoir, this setup corresponds to the case when bulk conditions (pressure or density) are not fixed. Although similar simulation setup is used very often in the literature [11], the laboratory measurements are performed usually under constant pressure conditions.

Three sets of information regarding the total fluid local density distribution, local ordering of the ends of the arms and the central beads of the SLM fluid have been extracted from these simulations. Figure 6 shows the trends in local density distributions of the THS/SLM fluid in a slit-like confinement at the different gap thickness. First of all, we see that total density in the slit behaves in a different manner than near a single wall. Namely, the wall density constantly increases when the slit becomes narrower that could reflect the flattening of the star-like aggregates against the wall and the layering is more pronounced. When the slit is narrowed up to three bead diameters, the number density of particles at the center of the

gap increased substantially. Since transformations in the density distributions of the ends of arms and the central beads are not so evident, it seems that the changes in the total density are due to the flexible nature of the star arms. In particular, for all considered separations between the slit walls, the ends of arms are enhanced at the walls while the central beads occupy the middle region of the pores.

3.3. Films formed from a star-like molecule fluid

In this subsection we show that properties of fluid films formed from the SLM aggregates could be studied within the FSA/SLM modeling as well. The local density distributions in the films composed of spherical molecules have been investigated by many authors and are now well understood both theoretically and experimentally [1]. In particular, it has been shown that well-defined layering in the films formed from simple fluids is the main reason for disjoining pressure and solvation force oscillations vs the film thickness. Here our aim is to obtain insight into the changes in the behavior of macroscopic properties of thin films due to the presence of SLM aggregates.

Theoretical modeling of the fluid film confinement. Now let us consider the surfaces of the slit pore that are not fixed and could move. To model such a case, we can imagine a huge reservoir filled with the SLM fluid having a particle number density, ρ. Into one part of this reservoir we immersed two planar surfaces that are infinite in area and are separated by the distance H. The material in between the surfaces will form the fluid film and is in equilibria with the reservoir fluid. To describe the interaction of the SLM species with a confinement, we assume that the surfaces of the immersed substrates are structureless walls located at $z = 0$ and $z = H$. The surfaces can attract or repel the adsorbed SLM particles. To model such an interaction we used the following fluid-wall potential:

$$U_{\mathrm{F}}(z,H) = \begin{cases} \infty, & \text{if} \quad z \leqslant 0 \quad \text{or} \quad z \geqslant H \\ \phi(z) + \phi(H-z), & \text{if} \quad 0 < z < H \end{cases}, \tag{3.8}$$

where z is the distance between the center of fluid particle and the film surface in the direction perpendicular to the surface. Such a form for the potential $U_{\mathrm{F}}(z,H)$ implies that the bead center can be located on the surface either at $z = 0$ or $z = H$ and the actual film thickness is $H + d$. The function $\phi(z)$ is modeled by the Lennard-Jones (9,3) potential:

$$\phi(z) = \epsilon_{\mathrm{W}} \left[\left(\frac{z_{\mathrm{W}}}{z} \right)^9 - \alpha \left(\frac{z_{\mathrm{W}}}{z} \right)^3 \right], \tag{3.9}$$

where parameters ϵ_{W} and z_{W} have the same meaning as for usual (12,6) Lennard-Jones potential, and switching parameter $\alpha = 0$ for repulsive film surfaces and $\alpha = 1$ for attractive film surfaces.

Local density distribution in the thick film. To calculate the local density distribution of the SLM fluid under the film confinement, similarly to the single-wall case, the associative version of the HAB integral equation is applied [39]. However, since the application of Perram procedure [36] is limited, at present, to the single-wall

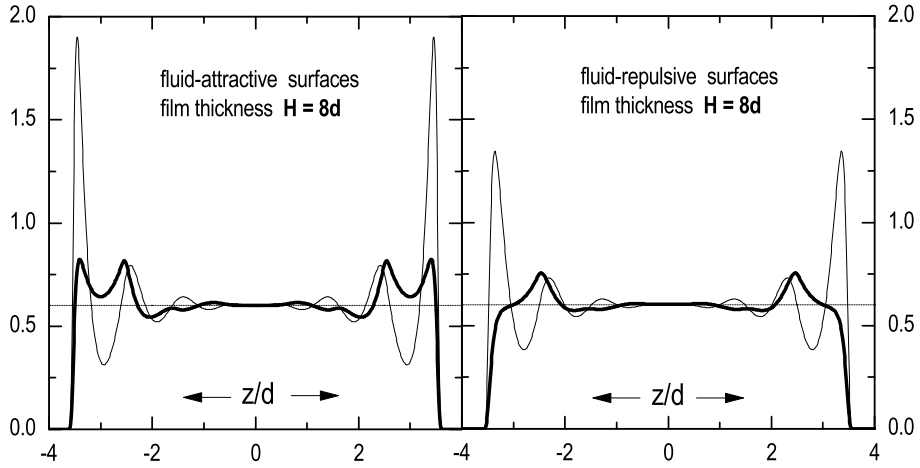

Figure 7. Normalized local density distribution of the FSA/SLM fluid in a film formed by fluid-attractive and fluid-repulsive confining surfaces.

case only, we used the direct iteration solution of the set of WOZ/APY equations in a form:

$$y_{j0}^{\alpha \mathrm{W}}(z,H) = \delta_{j0} + \sum_{lm} \sum_{\beta,\gamma} \int \mathrm{d}\mathbf{r}' c_{jl}^{\alpha\gamma}(r') \sigma_{lm}^{\gamma\beta} h_{m0}^{\beta \mathrm{W}}(|\mathbf{r} - \mathbf{r}'|, H), \tag{3.10}$$

but with the particle-wall interaction defined according to equation (3.8). The functions, $h_{i0}^{\alpha \mathrm{W}}(z,H)$ and $y_{i0}^{\alpha \mathrm{W}}(z,H)$, are the fluid-surface partial pair and cavity correlation functions, respectively. The total local density distribution in a film, $\rho_{\mathrm{F}}(z,H)$, is calculated as follows:

$$\rho_{\mathrm{F}}(z,H) = \rho\gamma(z,H) \left[y_{00}^{0\mathrm{W}}(z,H) + \frac{1}{\sigma_{\Gamma}^{\Gamma}} \sum_{i,\alpha} \sigma_i^{\alpha} y_{\Gamma-i,0}^{\Gamma-\alpha,\mathrm{W}}(z,H) \right], \tag{3.11}$$

where $\gamma(z,H)$ is the Boltzmann factor for the fluid-surface repulsion.

Some representative results for the local density distribution of the SLM fluid in films with attractive and repulsive surfaces are plotted in figure 7 as a function of separation from the surface. The film thickness is fixed at eight bead diameters. The local density is a convenient quantitative measure of the self-arrangement of the film fluid. Quite tall and narrow peaks that are observed in the immediate vicinity of the film surfaces reflect a well localized surface layer for spherical molecules. These peaks almost disappear for SLM fluids, especially in the case of the repulsive fluid-surface interaction. As the distance from the film surfaces increases, the magnitudes of the peaks decrease while their widths increase. There is a well-defined homogeneous region with the bulk density in the middle of the film that covers about one particle diameter for a fluid of spherical molecules but extends to approximately two diameters for the SLM fluid. This picture is nearly independent of the fluid-surface interaction. All this allows us to conclude that SLM fluid in the film tends to be separated from the film surfaces and becomes homogeneous faster because of the diminished influence of the confinement.

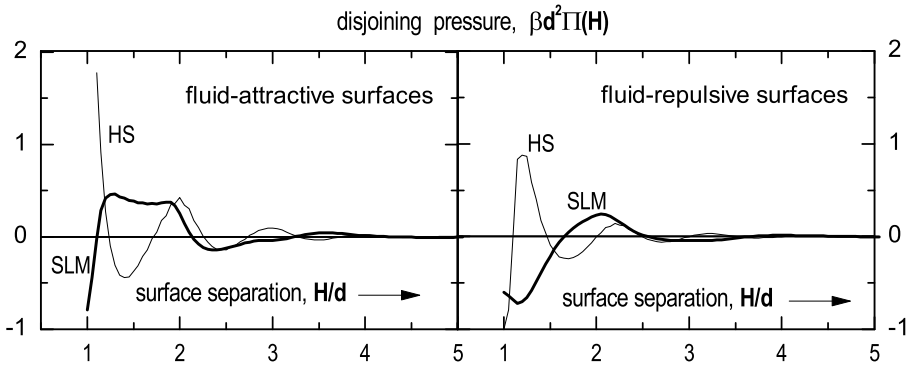

Figure 8. Structural disjoining pressure exerted by a film formed from the FSA/SLM fluid (thick solid line) and HS fluid (thin solid line) confined between two fluid-attractive and two fluid-repulsive surfaces.

Disjoining pressure. An important equilibrium property of any fluid confined to the film is the pressure, $P_N(H)$, exerted by confined fluid on the inner side of confining surfaces in the direction perpendicular to the surfaces. It can be calculated from the local density distribution in the film, $\rho_{\rm F}(z,H)$, as follows [41]:

$$P_N(H) = -\int_0^{H/2} \frac{\partial U_{\rm F}(z,H)}{\partial z}\rho_{\rm F}(z,H){\rm d}z. \tag{3.12}$$

The pressure $P_N(H)$, measured relative to the bulk pressure, $P_{\rm B}$, defines the so-called disjoining pressure:

$$\Pi(H) = P_N(H) - P_{\rm B}. \tag{3.13}$$

The bulk pressure, $P_{\rm B}$, is one of the parameters that determine the thermodynamic state of the SLM fluid in a bulk phase. It can be calculated independently or can be identified as a limiting value of the normal pressure acting between film surfaces at infinite separation. To satisfy the self-consistency of the numerical procedure we used the second possibility, i.e. we assume $P_{\rm B} \equiv P_N(H \to \infty)$.

Figure 8 shows the results of the WOZ/APY theory calculations of the disjoining pressure vs film thickness for the FSA/SLM fluid confined by attractive and repulsive surfaces. Disjoining pressure oscillates between positive and negative values and causes the confined SLM fluid to climb or spread on film surfaces. The differences in the amplitude, periodicity and decay of oscillations for confined HS fluid or confined FSA/SLM aggregates are evident. In reality this will influence the stability of the films formed from these two fluids, since the zeros of the disjoining pressure (surface separations at which the force exerted by the film fluid on the inner surfaces equals the bulk pressure on the outer side of the surfaces) are related to the stable or unstable thickness of fluid films.

Structural forces due to the SLM aggregates. To understand the qualitative trends in the film stability initiated by the architecture of the FSA/SLM aggregates we applied the approach known in colloid science as the Derjaguin approximation [1]. According to Derjaguin, the work per unit area, $W(H)$, to bring

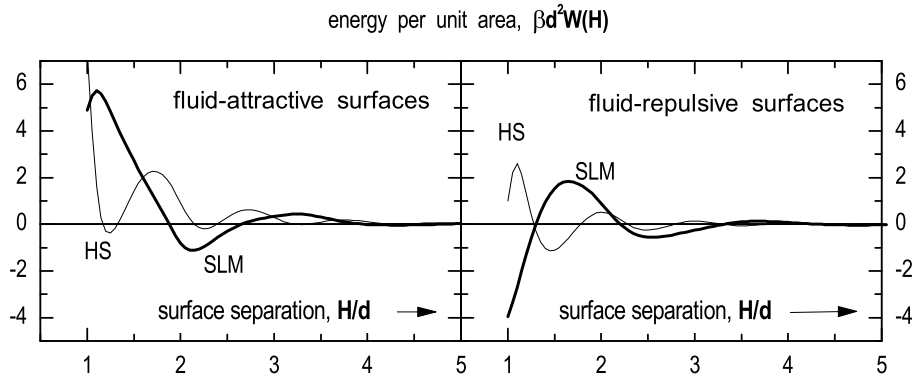

Figure 9. Structural energy per unit area between two fluid-attractive and two fluid-repulsive surfaces immersed into the FSA/SLM fluid (thick solid line) and HS fluid (thin solid line).

two film surfaces from infinity to the separation, H, can be calculated as

$$W(H) = \int_H^\infty \Pi(H')\mathrm{d}H'. \tag{3.14}$$

There is no direct interaction between two film surfaces and the energy, $W(H)$, is due to the structuring of the film fluid only, i.e. due to the so-called structural forces [42]. Since complexes in the FSA/SLM fluid are formed by tangent spheres, the extraction from $W(H)$ the similar quantity calculated for the HS monomers give us the information about the contribution into the film interaction of the energy induced by the shape of the SLM formations. Proceeding in this way, we found out [39] that the contribution due to the SLM shape is of the same order as the HS monomer result itself, however, it has an opposite sign and results in a decrease in the magnitude, shift in the phase, and increase in the periodicity of the oscillations of the force exerted by the SLM fluid film. The energy law observed in a HS fluid is modified switching to the SLM fluid (see figure 9). In general, the structural interaction energy is a damped oscillatory function of the film thickness, but with a periodicity different from that determined by the bead diameter. In contrast, the hard-sphere monomers are able to pack more efficiently and, due to this, fill in the space between the macrosurfaces down to very thickened films: range of oscillations observed in figure 9 is up to four particle diameters and the periodicity is approximately equal to the monomer diameter. The oscillations in the film formed from SLM fluid are weaker and periodicity increases to about two bead diameters. The structural interaction between film surfaces due to the SLM fluid at small film thickness (of the order of 1.5 bead diameter) is prevailed by the repulsive forces in the case when fluid-surface interaction is attractive, and promotes an attraction between the film surfaces when the fluid-surface interaction is repulsive. When the film thickness increases, the films formed from the SLM fluid stimulate attraction for both kinds of surfaces, though for the fluid attractive surfaces this effect is more pronounced.

Local density distribution and film stability. To understand why the SLM fluid tends to eliminate the structural force oscillations, we show in figure 10 the

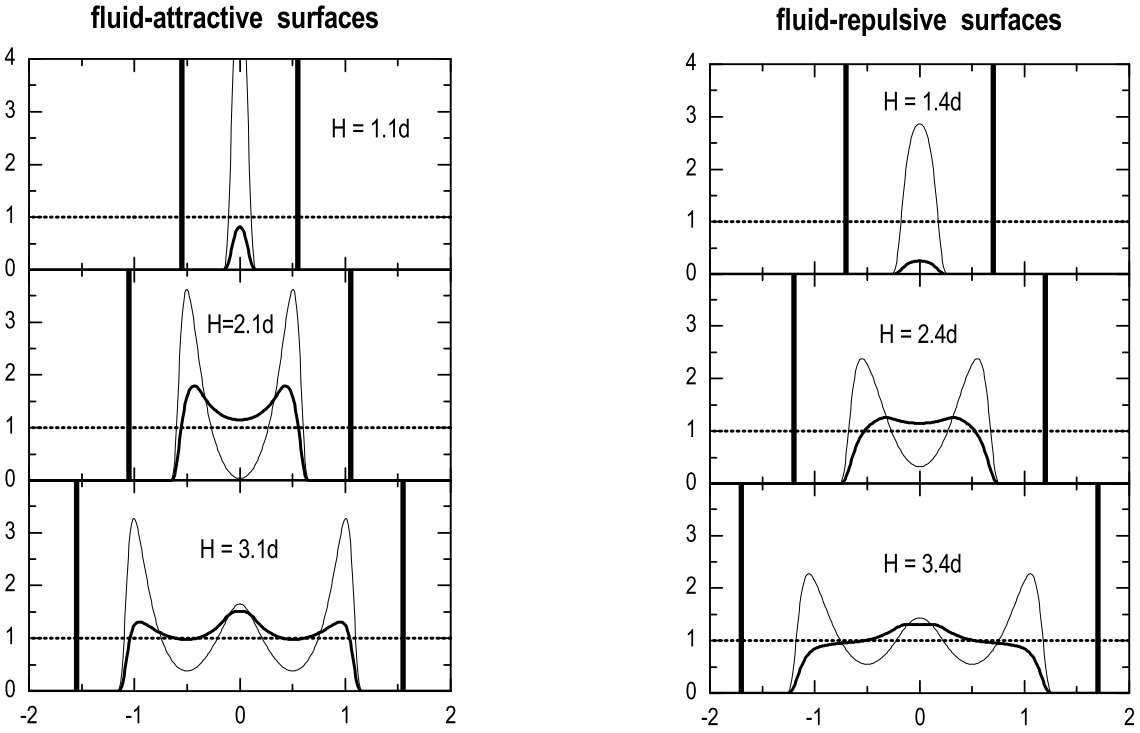

Figure 10. Local density distribution in the films formed from the FSA/SLM fluid (thick solid line) and HS fluid (thin solid line) between two attractive and two repulsive surfaces. Vertical thick lines indicate the position of film surfaces.

local density distributions across the films of the thicknesses determined from the energy law discussed in figure 9. Particularly, the film configurations (i.e., film thicknesses) that we chose to analyze in this figure roughly correspond to the film energy minima in the case of the film formed from the HS monomers. We see that a repulsive structural force between two fluid attractive surfaces at small separations between them originates from the presence of the surface layer of the SLM fluid and extends till the separations of the order of the thickness of this layer. For the surface separations intermediate between one and two bead diameters, the film fluid undergoes a local restructuring and the attraction between confining surfaces dominates. The existence of layering near film surfaces can be identified from the oscillations in a local density. This is a case of the film formed from spherical monomers. Two density maxima at a small film thickness, that we observe in the case of the SLM film, can be treated as a consequence of the spliting of a rather thick surface layer of the star aggregates; this layer remains disordered or amorphous. The local density in this film is always higher than the corresponding bulk density, and the force exerted by the film fluid on the film surfaces is repulsive. For the results discussed in figure 10 such a disordered first layer of the SLM film is extended until around three bead diameters. At this thickness the local density distribution starts to exhibit a relatively deep failure, that causes attraction between film boundaries. At a larger film thickness, the density distribution behaves as for the thick film discussed in figure 7.

4. Conclusions

In the present paper we discussed an application of the associative integral equation theory to the four-site model of associating fluids in order to study the properties of the star-like molecule fluids. We exploited the fact that the ideal network approximation, consisting in the neglect in the diagrammatic analysis of the intramolecular diagrams representing the formation of the loops and of the crossing rings, allows one to treat the problem analytically. Particularly, the analytical solution of the associative OZ integral equation within the associative PY closure, which we abbreviated as WOZ/APY theory, is available in literature [22–27].

There are at least two approaches to the star-like molecule fluids that are based on an associative hard-sphere model. One of them is discussed in the present issue by Kalyuzhnyi and Holovko [43]. These authors are using an analytical solution of the polymer Percus-Yevick approximation for the multicomponent mixture of associating hard spheres forming the star-like molecules in the limit of complete association. In contrast, in our contribution to describe the structure of the star fluid we have used the version of the four-site model of the associative fluid called as FSA/SLM model [40]. Despite its simple pair potential, the FSA/SLM model predicts a similar anomalous behavior for the structure factor [26] that is analogous to that observed by Likos *et al.* [2,3,12], i.e. the first peak decreases with increasing density while the second peak grows. To test and to justify our approach, we provide readers with comparison of the radial distribution functions and structure factors of the FSA/SLM model with MC simulation data for the tangent hard-sphere (THS/SLM) fluid model. Inhomogeneous star-like molecule fluids have been considered as well. Particularly, the density profiles of the star-like molecule fluids near a single wall and in the slit-like pore have been analyzed. Moreover, the FSA/SLM model within the framework of the WOZ/APY theory and associative version of the HAB approach was employed to probe the effect of the presence of star-like formations on the interaction between two macrosurfaces immersed into the SLM fluid. In many cases we found that the obtained results qualitatively reproduce important features reported from laboratory measurements.

Summarizing, we conclude that the considered FSA/SLM model of the star-like molecule fluid is qualitatively correct and exhibits the main features attributed to the star fluids. An application of the associative integral equation theory in the form of WOZ/APY realization to the case of a star-like molecule fluid is quite successful in the prediction of homogeneous structure ordering. It is noteworthy that the agreement of the WOZ/APY predictions and MC data is the best for a high density and the long arms, that is for the case of real star molecule fluids. We hope that the results and the insight we provided will stimulate both new theoretical and experimental studies in this field of macromolecular science.

5. Acknowledgement

YD was supported in part by the CONACyT of Mexico under Grant J32211-E.

References

1. Israelachvili J.N. Intermolecular and Surface Forces. New-York, Academic Press, 1992.
2. Likos C.N., Löwen H., Watzlawek M., Abbas B., Jucknischke O., Allgaier J., Richter D. // Phys. Rev. Lett., 1988, vol. 80, p. 4450.
3. Likos C.N., Löwen H., Poppe A., Willner L., Roovers J., Cubitt B., Richter D. // Phys. Rev. E, 1998, vol. 58, p. 6299.
4. Lekkerkerker H.N.W., Poon W.C.-K., Pusey P.N., Stroobants A., Warren P.B. // Europhys. Lett., 1992, vol. 20, p. 559.
5. Roovers J.E., Hadjichristidis N., Fetters L.J. // Macromolecules, 1983, vol. 16, p. 214.
6. Grest G.S., Kremer K., Witten T.A. // Macromolecules, 1987, vol. 20, p. 1376.
7. Grest G.S., Fetters L.J., Huang J.S., Richter D. // Adv. Chem. Phys., 1996, vol. 94, p. 67.
8. Zifferer G. // Macromol. Theory Simul., 1997, vol. 6, p. 381.
9. Sikorski A., Romiszowski P. // Macromol. Theory Simul., 1999, vol. 8, p. 103.
10. Lipson J.E.G., Whittington S.G., Wilkinson M.K., Martin J.L., Graunt D.S. // J. Phys. A: Math. Gen., 1985, vol. 18, p. L469.
11. Yethiraj A., Hall C.K. // Macromolecules, 1991, vol. 24, p. 709.
12. Watzlawek M., Löwen H., Likos C.N. // J. Phys.: Condens. Matter, 1998, vol. 10, p. 8189.
13. MacDowell L.G., Vega C. // J. Chem. Phys., 1998, vol. 109, p. 5681.
14. Yethiraj A., Hall C.K. // J. Chem. Phys., 1991, vol. 94, p. 3943.
15. von Ferber C., Holovatch Y. // Physica A, 1998, vol. 249, p. 327.
16. Alessandrini J.L., Carignano M.A. // Macromolecules, 1992, vol. 25, p. 1157.
17. Cherayil B.J., Bawendi M.G., Miyake A., Freed K.F. // Macromolecules, 1986, vol. 19, p. 2770.
18. Sear R., Jackson G. // Molec. Phys., 1994, vol. 81, p. 801.
19. Daoud M., Cotton J.P. // J. Phys. (France), 1982, vol. 43, p. 531.
20. Kalyuzhnyi Yu. // Condens. Matter Phys., 1997, No. 10, p. 51.
21. Yethiraj A., Curro G., Rajasekaran J.J. // J. Chem. Phys., 1995, vol. 103, p. 2229.
22. Wertheim M.S. // J. Stat. Phys., 1986, vol. 42, p. 459.
23. Wertheim M.S. // J. Stat. Phys., 1986, vol. 42, p. 477.
24. Chang J., Sandler S. // J. Chem. Phys., 1995, vol. 102, p. 437.
25. Chang J., Sandler S. // J. Chem. Phys., 1995, vol. 103, p. 3196.
26. Vakarin E., Duda Yu., Holovko M.F. // Molec. Phys., 1997, vol. 90, No. 4, p. 611.
27. Vakarin E., Duda Yu., Holovko M.F. // J. Stat. Phys., 1997, vol. 88, p. 1333.
28. Vakarin E., Holovko M.F., Duda Yu. // Molec. Phys., 1997, vol. 91, No. 2, p. 203–214.
29. Duda Yu., Segura C.J., Vakarin E., Holovko M.F., Chapman W. // J. Chem. Phys., 1998, vol. 108, p. 9168.
30. Baxter R.J. // J. Chem. Phys., 1968, vol. 49, p. 2770.
31. Duda Yu. // J. Chem. Phys., 1998, vol. 109, p. 9015.
32. Wertheim M.S. // J. Math. Phys., 1964, vol. 5, No. 3, p. 643–654.
33. Duda Yu., Millan-Malo B., Pizio O., Henderson D. // J. Phys. Studies, 1997, vol. 1, p. 45.
34. Dickman R., Hall C.K. // J. Chem. Phys., 1988, vol. 89, p. 3168.
35. Metropolis N.A., Rosenbluth A.W., Rosenbluth M.N., Teller A.H., Teller E. // J. Chem. Phys., 1953, vol. 21, p. 1087.

36. Perram J.W. // Molec. Phys., 1975, vol. 30, p. 1505.
37. Trokhymchuk A., Henderson D., Sokolowski S. // Canadian J. Physics, 1996, vol. 74, p. 65.
38. Henderson D., Abraham F.F., Barker J.A. // Molec. Phys., 1976, vol. 31, No. 6, p. 1291.
39. Duda Yu., Henderson D., Trokhymchuk A., Wasan D. // J. Phys. Chem., 1999, vol. 103, p. 7495.
40. Duda Y., Garcia I., Trokhymchuk A., Henderson D. // Molec. Phys., 2000, vol. 98, No. 17, p. 1287.
41. Henderson D., Blum L., Lebowitz J.L. // J. Electroanal. Chem., 1979, vol. 102, p. 315.
42. Trokhymchuk A., Henderson D., Nikolov A., Wasan D.T. // Langmuir, 2001, vol. 17, No. 16, p. 4940.
43. Kalyuzhnyi Yu.V., Holovko M.F. // Condens. Matter Phys., 2002, vol. 5, No. 2, p. 211.

Про один спрощений підхід до опису рідин зіркових молекул

Ю.Дуда [1,2] , А.Трохимчук [2,3]

[1] Відділ молекулярної інженерії, Мексиканський інститут нафти, Мехіко, Мексика

[2] Інститут фізики конденсованих систем НАН України, 79011 Львів, вул. Свєнціцького, 1

[3] Факультет хімії та біохімії, Університет Брайхем Янґ, Прово, UT 84602, США

Отримано 29 березня 2002 р.

Запропоновано теоретичний підхід до вивчення широкого спектру рівноважних властивостей рідин, молекули яких мають форму зірок (як наприклад полістирен, та ряд кополімерів). Підхід у своїй основі ґрунтується на аналітичному розв'язку, отриманому в теорії інтегральних рівнянь для так званої асоціативної моделі силових центрів. Результати та висновки з теоретичного підходу підкріплені порівняннями з комп'ютерним експериментом, проведеним для моделі гнучких полімерів, що мають форму зірок. Показано, що запропонований теоретичний підхід працює добре для однорідної фази, де добре відтворює структурний фактор для відносно довгих кінцівок зірки і високих густин рідини. Отримані результати відтворюють найважливіші характеристики сольватаційної сили між двома плоскими поверхнями, зануреними у розчин з наявними зірковими молекулами, що спостерігається у лабораторному експерименті.

Ключові слова: *зіркові молекули, асоціативна теорія інтегральних рівнянь, комп'ютерний експеримент*

PACS: *05.20.Jj, 61.25.Em*